

EVOLUTION OF HELIUM STARS

RICHARD STOTHERS AND CHAO-WEN CHIN

Institute for Space Studies, Goddard Space Flight Center

Received 1977 January 20

ABSTRACT

The evolution of helium stars in the mass range 4–15 M_{\odot} has been followed from the initial helium main sequence to the end of carbon burning in the core, with the use of Carson's new radiative opacities. As compared with earlier work based on smaller opacities, the main-sequence band in the H-R diagram is now both wider and cooler than before. If neutrino losses are neglected in the stellar models, the phase of carbon burning in the core occurs in the red-supergiant region; otherwise, it occurs, as it does in the earlier models with or without neutrino emission, close to the helium main sequence. Observational data for Wolf-Rayet stars and R Coronae Borealis variables are found to lend some support to the new models.

Subject headings: opacities — stars: evolution — stars: interiors

I. INTRODUCTION

The interior of a helium star is so hot that electron scattering has long been thought to dominate the radiative opacity at every layer. However, at temperatures around a million degrees and at very low densities, Carson's (1976) recent opacity calculations have indicated the existence of a large "bump" in the opacity curve due to the ultimate ionization of the CNO elements—apparently a result of his adoption of the hot "Thomas-Fermi" model of the atom for the metals, whereas previous opacity calculations have mostly been based on a "hydrogenic" model. In models of stars lying on the helium main sequence, the new opacity bump has been found to produce a striking expansion of the outer envelope of the star for masses exceeding $\sim 4 M_{\odot}$ (Stothers 1976).

The purpose of the present paper is to complete the calculation of the main-sequence phase of evolution for massive helium stars based on the new opacities and to pursue the evolutionary calculations up to the end of carbon burning in the core. A comparison of the theoretical models with observational data will conclude the paper.

II. ASSUMPTIONS

The adopted stellar masses are 2, 4, 8, and 15 M_{\odot} . Initial metals abundances are $Z_e = 0.02$ and $Z_e = 0.04$. Evolution beyond the end of helium burning at the center has been computed with and without the inclusion of neutrino emission, which begins to become important during the onset of central carbon burning. For 2 M_{\odot} , the carbon-burning phase has not been calculated, as the electron gas would be degenerate in the stellar core for this case. Methods and input physics used to construct the stellar models are the same as those described previously (Stothers and Chin 1973*a, b*), with the exception of the following parameters.

Opacities.—Carson's new radiative opacities are used everywhere in the star except in the atmosphere. They are used in tabular form if $3.85 < \log T < 7.80$, but in the following analytic form for higher temperatures:

$$\kappa = 0.2(1 + 1.5T_9)^{-1} + 7.2 \times 10^{-8} \left(\sum_i Z_i^2 X_i A_i^{-1} \right) (\rho/\mu_E)^{0.7} T_9^{-3.2},$$

where $T_9 = T \times 10^9$ and cgs units apply. In this formula, A_i , Z_i , and X_i are respectively the relative atomic mass, charge, and abundance by mass of species i ; and $\mu_E = 2$. The first term in the formula represents the contribution from scattering by free electrons, modified by the relativistic correction and various other corrections; and the second term contains the contribution from atomic absorption, cast into the form of a modified Kramers law. This formula fits Carson's opacity tables in the nondegenerate high-temperature region to within 5%. The absorption part of the formula turns out to be almost identical to a formula fitted by Larson (Morris and Demarque 1966) to earlier "hydrogenic" opacity tables. The scattering part is somewhat larger than the scattering formula given by Deinzer and Salpeter (1965), based on Sampson's (1959) computations. But, on the whole, for $\log T > 6.5$, Carson's opacities are not very different from earlier opacities, as long as the density is low.

Convection.—In the present work Schwarzschild's criterion for convection has been adopted, and the convectively unstable layers are assumed to mix homogeneously. Semiconvection has been ignored. In practice, homogeneous mixing is a fairly good assumption here since convection does not break out in any layers with a significant gradient of mean molecular weight, except, occasionally, just beyond the edge of the shrinking convective core during the last stages of

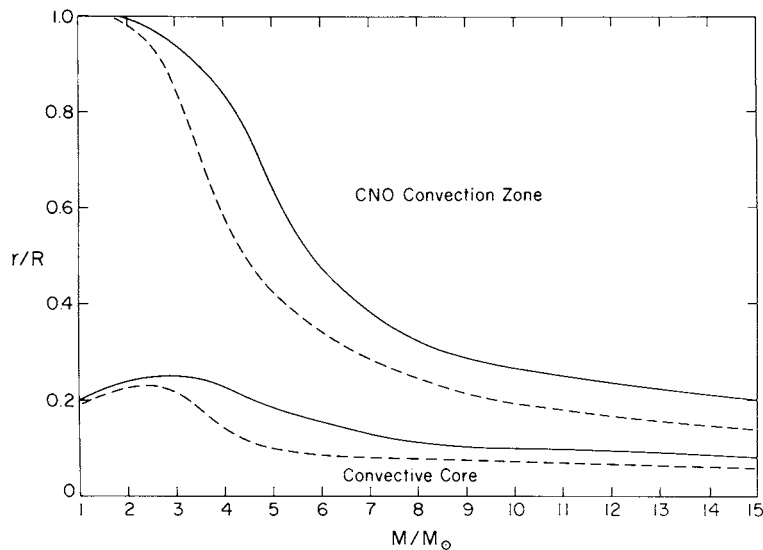


FIG. 1.—Spatial extent of the convective zones in unevolved models of helium stars. Solid and dashed lines refer to the convective boundaries for metals abundances of $Z_e = 0.02$ and $Z_e = 0.04$, respectively. Note that the radius fraction of the convective core is not monotonic with increasing stellar mass (however, the mass fraction is) and that the radius fraction of the CNO convection zone grows with increasing stellar mass (however, the mass fraction of this zone remains negligibly small). The effect on the zonal boundaries of changing the adopted value of α_p by a factor f is roughly equivalent to the effect of changing Z_e by a factor f^{-1} .

core helium burning. Special attention has been paid to determining the precise boundary of the convective core. For this purpose we have adopted (1) a smooth opacity formula (given above) across the boundary; (2) small time steps and fine mass zoning; and (3) a strict requirement that the radiative and adiabatic temperature gradients be exactly equal to each other on the inside edge of the chemical discontinuity which forms at the convective core boundary, and that all the underlying layers be actually convective. These procedures have essentially eliminated (except at $2 M_\odot$) the fluctuations of the core boundary that have usually been found in stellar models near the end of core helium burning (e.g., Paczyński 1971; Savonije and Takens 1976). In the nonadiabatic convective layers close to the surface of the star, the mixing length has been set equal to the local pressure scale height ($\alpha_p = 1$); these layers contain the moderately thick CNO ionization zone on the helium main sequence, as

shown in Figure 1, and the very thick helium ionization zone in the red-supergiant models.

Neutrino emission.—The rate of energy loss due to neutrino emission has been taken from Beaudet, Petrosian, and Salpeter (1967) in the form of a detailed fitted formula.

III. THEORETICAL EVOLUTIONARY TRACKS

Stellar models covering the main helium-burning phase of evolution are presented in Table 1 for the following three stages: (1) zero-age main-sequence stage,¹ (2) stage where the effective temperature attains a minimum (except at $2 M_\odot$, where the minimum is attained shortly after the zero-age stage), and (3) stage

¹ Moderate differences between these models and previously published models based on the same opacities are due to differences in the adopted nuclear reaction rates and in choices of α_p .

TABLE 1
SELECTED EVOLUTIONARY MODELS OF HELIUM STARS

| M/M_\odot | Z_e | MODEL 1 | | | | | MODEL 2 | | | | MODEL 3 | | | |
|-------------|-------|---------|-------------------|------------|-------------------------|--|---------|-------------------|------------|-------------------------|---------|-------------------|------------|-------------------------|
| | | Y_c | $\log(L/L_\odot)$ | $\log T_e$ | $\tau(10^5 \text{ yr})$ | | Y_c | $\log(L/L_\odot)$ | $\log T_e$ | $\tau(10^5 \text{ yr})$ | Y_c | $\log(L/L_\odot)$ | $\log T_e$ | $\tau(10^5 \text{ yr})$ |
| 2..... | 0.02 | 0.980 | 3.361 | 4.836 | 0.00 | | 0.042 | 3.583 | 4.865 | 29.23 | 0.0 | 3.675 | 4.928 | 30.90 |
| 2..... | 0.04 | 0.960 | 3.356 | 4.824 | 0.00 | | 0.039 | 3.570 | 4.839 | 28.53 | 0.0 | 3.665 | 4.871 | 30.14 |
| 4..... | 0.02 | 0.980 | 4.206 | 4.899 | 0.00 | | 0.044 | 4.413 | 4.795 | 10.76 | 0.0 | 4.493 | 4.799 | 11.50 |
| 4..... | 0.04 | 0.960 | 4.207 | 4.798 | 0.00 | | 0.041 | 4.415 | 4.721 | 10.56 | 0.0 | 4.490 | 4.727 | 11.25 |
| 8..... | 0.02 | 0.980 | 4.916 | 4.778 | 0.00 | | 0.047 | 5.097 | 4.715 | 5.87 | 0.0 | 5.159 | 4.733 | 6.30 |
| 8..... | 0.04 | 0.960 | 4.918 | 4.711 | 0.00 | | 0.046 | 5.094 | 4.608 | 5.63 | 0.0 | 5.151 | 4.635 | 6.06 |
| 15..... | 0.02 | 0.980 | 5.448 | 4.735 | 0.00 | | 0.053 | 5.585 | 4.660 | 3.97 | 0.0 | 5.627 | 4.695 | 4.31 |
| 15..... | 0.04 | 0.960 | 5.450 | 4.658 | 0.00 | | 0.013 | 5.599 | 4.491 | 4.10 | 0.0 | 5.626 | 4.491 | 4.20 |

NOTE.—In all cases $\alpha_p = 1$.

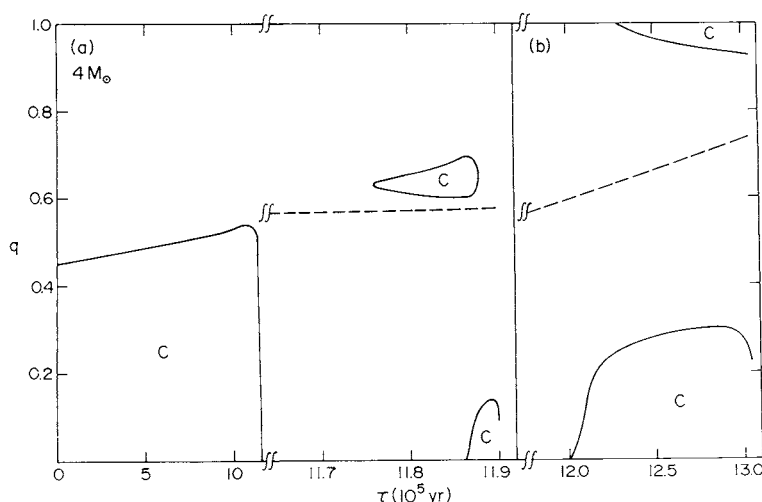


FIG. 2.—Evolution of the structural zones of a helium star of $4 M_{\odot}$ with $Z_e = 0.02$. Convective zones are indicated by the letter C. The dashed line represents the peak of the helium-burning shell. The ordinate is mass fraction q , and the abscissa is time. Panel *a* is divided into two segments, which include (1) core helium burning and (2) core carbon burning with neutrino emission included. Panel *b* covers the alternate case of core carbon burning without neutrino emission.

where the central helium content falls to zero. The interior structural evolution is shown in Figures 2, 3, and 4 for the three highest masses; the zonal boundaries are found not to be very sensitive to the choice of initial metals abundance when the mass fraction rather than the radius fraction is plotted.

At each stellar mass the convective core expands by nearly the same amount (0.10 in mass fraction) during the course of central helium burning. When the helium content at the center drops to $Y_c \approx 0.04$, the convective core boundary begins to recede smoothly toward the center. These results are qualitatively similar to results obtained by Paczyński (1971) and Savonije and Takens (1976), except for the erratic behavior of the convective core boundary in their models with small Y_c . However, in models where the initial metals

abundance is negligibly small, the amount of core growth seems to be either slight (Deinzer and Salpeter 1964; Divine 1965) or entirely absent (Sugimoto 1970; Arnett 1972*a, b*; Nomoto 1974).

When helium is completely exhausted at the center, convection vanishes simultaneously, and the core undergoes a rapid contraction. With core temperatures everywhere rising, the helium-rich periphery of the core (the former maximum extent of core convection) ignites and develops into a shell source of energy generation. Due to the increased flux of energy poured into the envelope, a convective region forms immediately above the shell source.

Further evolution of the models is governed by the presence or absence of neutrino emission. When neutrino losses are not included in the models, the

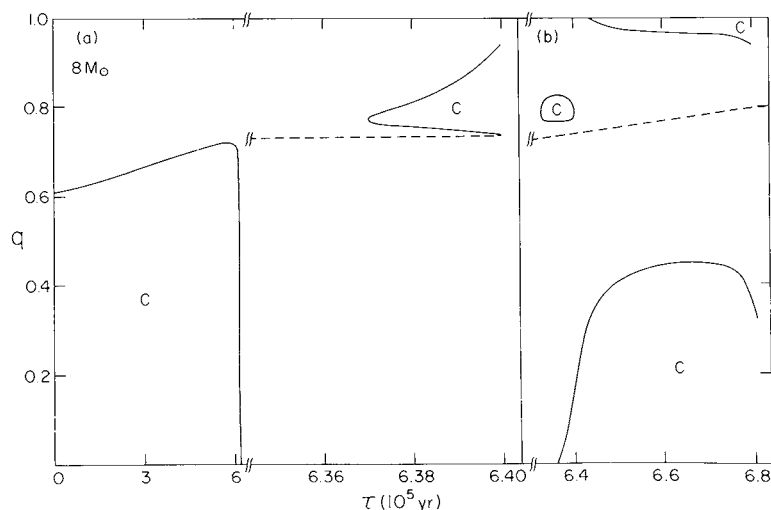


FIG. 3.—Evolution of the structural zones of a helium star of $8 M_{\odot}$ with $Z_e = 0.02$. Coding is the same as in Fig. 2.

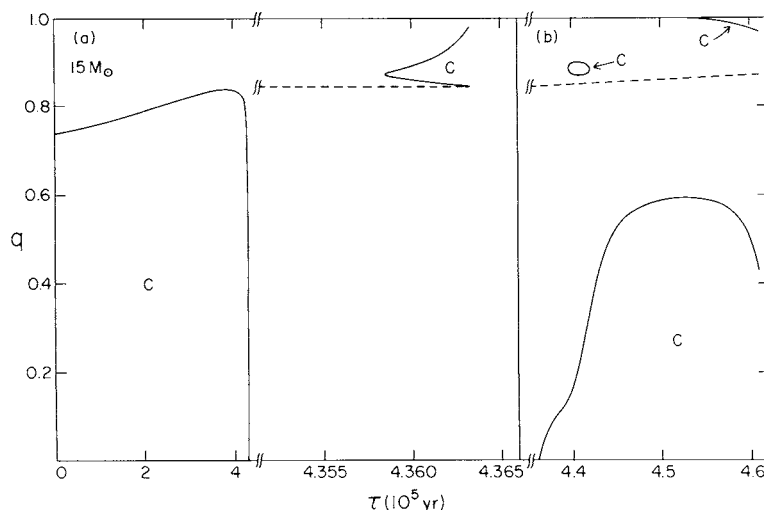


FIG. 4.—Evolution of the structural zones of a helium star of $15 M_{\odot}$ with $Z_e = 0.02$. Coding is the same as in Fig. 2.

lifetime is relatively long, and carbon burns steadily in a well-developed convective core. Since the helium shell source eventually burns its way out to cooler layers, the overlying convective region finally disappears. On the other hand, when neutrino losses are taken into account, the evolutionary time scale quickly accelerates to the point where it approaches the hydrodynamical collapse time, shortly before carbon is exhausted at the center. The heavy energy drain in the form of neutrino emission robs the stellar photon field chiefly near the center, flattens (later inverts) the local temperature gradient, and suppresses core convection entirely in the models for 8 and $15 M_{\odot}$. Violent

contraction of the outer part of the core accompanies the burning of carbon in the inner part and causes the infalling helium shell to heat up rather more in the case with neutrino emission than in the case without it. As a result, the energy flux deposited in the envelope is significantly enlarged when neutrino emission is included, so that the convective region immediately above the burning shell actually grows as time goes on.

The phase of carbon depletion in the core has also been calculated for massive helium stars by Sugimoto (1970), Paczyński (1971), Arnett (1972*b*), and Nomoto (1974), with results in qualitatively good agreement with ours, despite the considerable differences in the

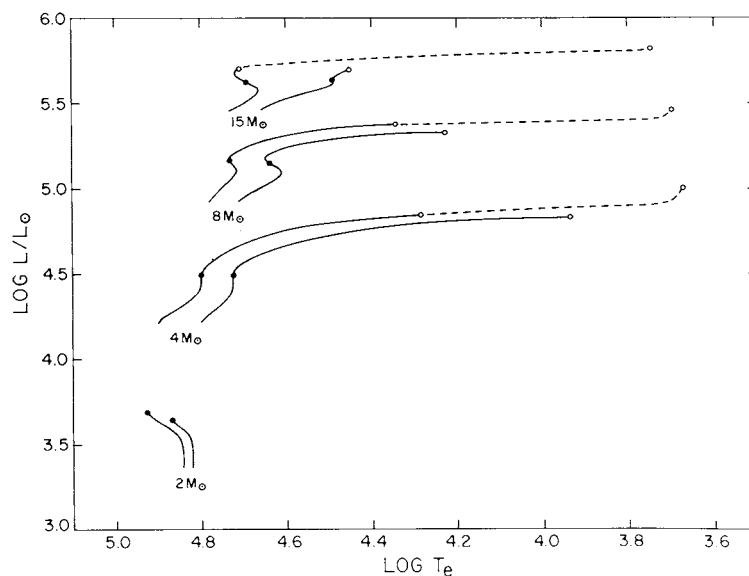


FIG. 5.—Theoretical evolutionary tracks in the H-R diagram for helium stars of 2, 4, 8, and $15 M_{\odot}$. The hotter and cooler of the two sequences at each mass refer, respectively, to $Z_e = 0.02$ and $Z_e = 0.04$. Symbols have the following meanings: *dot*, end of core helium burning; *circle*, end of core carbon burning; *dashed line*, carbon burning without neutrino emission.

carbon-to-oxygen ratios and nuclear reaction rates. Thermal pulses in the helium-burning shell, if they are present at all, are certain to be unimportant from an evolutionary standpoint (Stothers and Chin 1973b).

On the H-R diagram the tracks representing the new evolutionary sequences show a considerable variety of forms (see Fig. 5). In contrast, the older tracks, based on "hydrogenic" opacities, exhibit very nearly the same form at all masses as the present tracks for $2 M_{\odot}$. Moreover, these older tracks define a very narrow "main-sequence" band that slopes monotonically toward higher luminosities and effective temperatures in the H-R diagram (e.g., Paczyński 1971). But the main-sequence band for the new tracks begins to widen and to slope toward cooler effective temperatures for luminosities greater than about $10^4 L_{\odot}$ (i.e., for masses greater than $\sim 4 M_{\odot}$).

In the older models, the phase of carbon burning occurs close to the helium main-sequence band in the H-R diagram for masses greater than $\sim 2 M_{\odot}$, whether or not neutrino emission is included in the models (Paczynski 1971). In the present models, however, Carson's large opacities expand the outer envelope of the star to red-supergiant dimensions if the evolutionary time scale is long enough, i.e., if it is longer than the envelope Kelvin time. This condition occurs only in the absence of neutrino emission.² Since the characteristic effective temperature of a helium-rich red supergiant is higher than that of its hydrogen-rich counterpart, the outer convective envelope does not penetrate very deeply into the interior of a helium star, and so does not produce a carbon star by mixing carbon upward to the surface.

It should be mentioned that our final carbon-to-oxygen ratios generated by core helium burning are quite small (as a result of our particular choice of the nuclear reaction rates for helium burning). However, the specification of a larger final carbon-to-oxygen ratio is found to make virtually no difference in the evolutionary tracks, because, in the absence of neutrino emission, the red-supergiant configuration is found to be definitely attained in any case, while, in the presence of neutrino emission, the time scale for depleting the

² In the case of stellar masses less than $\sim 2 M_{\odot}$ it is only the models *with* neutrino emission that develop very extended envelopes (Paczynski 1971).

carbon is always much shorter than the envelope Kelvin time. Lifetimes for the carbon-burning phase are given in Table 2, where τ_C/τ_{He} is the ratio of the carbon-burning lifetime (as measured from the instant of vanishing central helium content) to the lifetime of core helium burning, and τ_{red}/τ_{He} is the ratio of the amount of time spent at effective temperatures cooler than $\log T_e = 4.0$ to the lifetime of core helium burning.

IV. COMPARISON WITH OBSERVATIONS

Helium-rich stars of high mass are known to exist in nature, and a few of them belong to a subclass of Wolf-Rayet stars that seem to contain no detectable hydrogen (spectral type WN5). Their approximate position in the H-R diagram is indicated in Figure 6, and their masses are, on the average, $\sim 14 M_{\odot}$ (data from Smith 1973). That atmospheric abundance ratios N/C appear to be quite large suggests that the material has been processed through the CNO bi-cycle in an earlier phase of evolution before the hydrogen envelope was lost. Although Carson's opacities, which have been used in our theoretical stellar models, are based on a solar N/C ratio, nevertheless the main features of his large CNO opacity bump would probably remain about the same for any other relative distribution of these elements, since the relevant ultimate ionization potentials are approximately the same. Therefore, it would appear that our predicted main-sequence band for helium stars can readily account for the observed location of WN5 stars in the H-R diagram (for a fuller discussion, see Stothers 1976).

The only cool helium stars that are known at present are R Coronae Borealis variables. Two variables of this class have been suggested as being massive stars and as belonging to young stellar associations with known distances: ρ Cas near IV Cas (Bidelman 1958; Sargent 1961; Schmidt-Kaler 1961) and the Sanduleak-Seggewiss object near NGC 6231 (Bessell *et al.* 1970; Milone 1973). However, membership of these two objects in the associations indicated and in the general class of helium stars has been very seriously questioned (for ρ Cas: Payne-Gaposchkin 1963; for the Sanduleak-Seggewiss object: Herbig 1972; Knacke, Strom, and

TABLE 2
LIFETIME OF HELIUM STARS DURING THE PHASE OF CORE CARBON BURNING

| M/M_{\odot} | Z_e | Initial Core Carbon Abundance | Neutrino Emission | τ_C/τ_{He} | τ_{red}/τ_{He} |
|---------------|-------|-------------------------------------|----------------------|--------------------|------------------------|
| 4..... | 0.02 | 0.23 | no | 0.140 | 0.081 |
| | | | yes | 0.035 | ... |
| 4..... | 0.04 | 0.22 | yes | 0.035 | 0.004 |
| 8..... | 0.02 | 0.17 | no | 0.097 | 0.062 |
| | | | yes | 0.016 | ... |
| 8..... | 0.04 | 0.17 | yes | 0.019 | ... |
| 15..... | 0.02 | 0.10 | no | 0.071 | 0.042 |
| | | | yes | 0.012 | ... |
| 15..... | 0.04 | 0.10 | yes | 0.012 | ... |

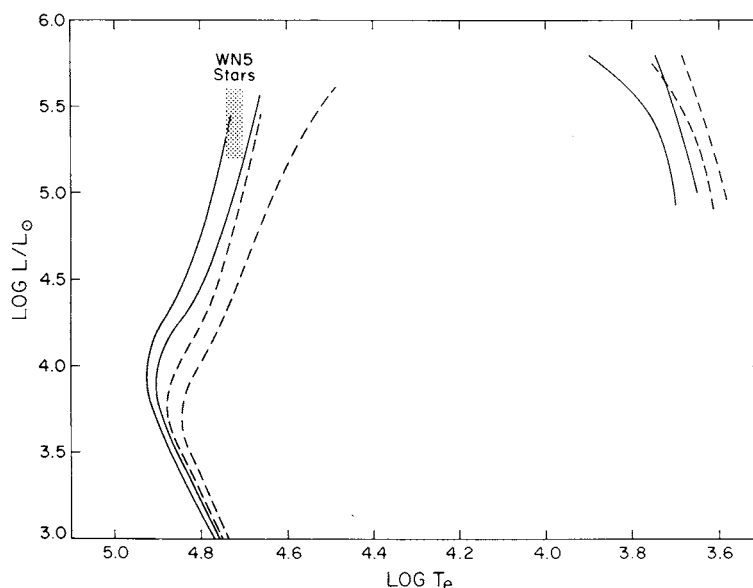


FIG. 6.—Theoretical main-sequence bands in the H-R diagram for helium stars with $Z_e = 0.02$ (solid lines) and $Z_e = 0.04$ (dashed lines). The segments at low effective temperature refer only to massive helium stars of $4\text{--}15 M_\odot$ in the slow stages of carbon burning without neutrino emission. A value of $\alpha_p = 1$ has been adopted for the stellar models; a larger (smaller) value would systematically increase (decrease) the effective temperatures of all the models.

Strom 1973; Milone 1973). Since the luminosities of other R Coronae Borealis stars are not known to exceed $\sim 10^4 L_\odot$ (Feast 1975), it is likely that massive cool helium stars are either extremely rare or absent.

The theoretically expected number of these stars is easy to estimate. Assuming that carbon and oxygen are about equally abundant at the end of central helium burning and allowing nucleosynthesis to proceed all the way to iron formation in the core, we may predict a ratio of cool-to-hot helium stars of high mass equal to 0 (neutrino emission included) or to ~ 0.4 (neutrino emission neglected). However, the

observed group of hot helium stars is simply too small to conclude that neutrino emission is favored by the observed paucity of cooler objects. When better information is available on the possibility of helium overabundances in some “ordinary” cool supergiants, a more substantial comparison with all the Wolf-Rayet stars (regardless of their surface hydrogen abundances) can be made.

We thank T. Richard Carson for allowing us to use his new radiative opacities in advance of their publication.

REFERENCES

- Arnett, W. D. 1972a, *Ap. J.*, **176**, 681.
 ———. 1972b, *Ap. J.*, **176**, 699.
 Beaudet, G., Petrosian, V., and Salpeter, E. E. 1967, *Ap. J.*, **150**, 979.
 Bessell, M. S., Rodgers, A. W., Eggen, O. J., and Hopper, P. B. 1970, *Ap. J. (Letters)*, **162**, L11.
 Bidelman, W. P. 1958, *IAU Symposium No. 5, Comparison of the Large-Scale Structure of the Galactic System with that of Other Stellar Systems*, ed. N. G. Roman (Cambridge: University Press), p. 54.
 Carson, T. R. 1976, *Ann. Rev. Astr. Ap.*, **14**, 95.
 Deinzer, W., and Salpeter, E. E. 1964, *Ap. J.*, **140**, 499.
 ———. 1965, *Ap. J.*, **142**, 813.
 Divine, N. 1965, *Ap. J.*, **142**, 824.
 Feast, M. W. 1975, *IAU Symposium No. 67, Variable Stars and Stellar Evolution*, ed. V. Sherwood and L. Plaut (Dordrecht: Reidel), p. 129.
 Herbig, G. H. 1972, *Ap. J. (Letters)*, **174**, L89.
 Knacke, R. F., Strom, K. M., and Strom, S. E. 1973, *Ap. J.*, **179**, 493.
 Milone, L. A. 1973, *Ap. J.*, **180**, 631.
 Morris, S. C., and Demarque, P. 1966, *Zs. f. Ap.*, **64**, 238.
 Nomoto, K. 1974, *Progr. Theoret. Phys. (Kyoto)*, **52**, 453.
 Paczyński, B. 1971, *Acta Astr.*, **21**, 1.
 Payne-Gaposchkin, C. 1963, *Ap. J.*, **138**, 320.
 Sampson, D. H. 1959, *Ap. J.*, **129**, 734.
 Sargent, W. L. W. 1961, *Ap. J.*, **134**, 142.
 Savonije, G. J., and Takens, R. J. 1976, *Astr. Ap.*, **47**, 231.
 Schmidt-Kaler, T. 1961, *Zs. f. Ap.*, **53**, 1 and 28.
 Smith, L. F. 1973, *IAU Symposium No. 49, Wolf-Rayet and High Temperature Stars*, ed. M. K. V. Bappu and J. Sahade (Dordrecht: Reidel), p. 15.
 Stothers, R. 1976, *Ap. J.*, **209**, 800.
 Stothers, R., and Chin, C.-w. 1973a, *Ap. J.*, **179**, 555.
 ———. 1973b, *Ap. J.*, **182**, 209.
 Sugimoto, D. 1970, *Progr. Theoret. Phys. (Kyoto)*, **44**, 599.

CHAO-WEN CHIN and RICHARD STOTHERS: Institute for Space Studies, Goddard Space Flight Center, NASA, 2880 Broadway, New York, NY 10025